Contents list avilable at CBIORE journal website

International Journal of Renewable Energy Development

Journal homepage: https://ijred.cbiore.id

Research Article

Bi-directional modulation of electron transfer and capacitive behavior in sediment microbial fuel cells by hydrochar and acetate

Marcelinus Christwardana[a,b,c,*], Yayuk Astuti[a], H. Hadiyanto[d,e], Achmad Yanuar Maulana[f,g], K. Khoirunnisa[a], Dilla Dayanti[b,c], Keisya Natania Nur A'intan[a]

[a]*Department of Chemistry, Faculty of Science and Mathematics, Diponegoro University, Indonesia*

[b]*Master Program of Energy, School of Postgraduate Studies, Diponegoro University, Indonesia*

[c]*Research Collaboration Center for Electrochemistry, BRIN - Diponegoro University, Indonesia*

[d]*Department of Chemical Engineering, Faculty of Engineering, Diponegoro University, Indonesia*

[e]*Center of Biomass and Renewable Energy (CBIORE), UPT Lab Terpadu 4th Floor, Diponegoro University, Indonesia*

[f]*Department of Chemistry, Dong-A University, Busan 49315, South Korea*

[g]*DAU G-LAMP Project Group, Institute of Natural Science, Dong-A University, Busan, 49315, South Korea*

Abstract. Marine sediment microbial fuel cells (MS-MFCs) provide a sustainable approach for harvesting energy from benthic environments, but their performance is limited by slow electron-transfer kinetics, unstable power output, and charge-storage capability. This study investigates the coupled kinetic and capacitive enhancement of MS-MFCs through co-modification with biomass-derived hydrochar (HC) and acetate as complementary electron-transfer and metabolic modulators. Four sediment compositions containing 0, 5, 10, and 15% (v/v) HC were operated for 30 days under a 1 kΩ external load, with acetate introduced on Day 21 to stimulate microbial metabolism. Electrochemical behavior was evaluated using cyclic voltammetry, electron-transfer kinetic analysis, current-density monitoring, power-density measurements, and physicochemical characterization of the anolyte. The apparent electron-transfer rate constant (k_s) increased from 1.77 s^{-1} in the unamended control to 3.19 s^{-1} and 3.49 s^{-1} in the 10% and 15% HC systems, respectively. Maximum power densities reached 21.8–23.1 mW m^{-2}, approximately three orders of magnitude higher than the control. Hydrochar also improved redox stability, ionic conductivity, and apparent capacitive behavior by providing a porous, conductive, and pseudocapacitive scaffold that supported microbial attachment and facilitated microbe–electrode coupling. Meanwhile, acetate served as a readily metabolizable carbon source that accelerated microbial activity and enhanced electron delivery to the anode. The strongest performance was observed at 10–15% HC, although the 15% system showed mass-transfer limitations during operation. These findings demonstrate a synergistic relationship between kinetic enhancement, substrate utilization, and capacitive charge buffering, offering a mechanistic basis for designing robust, self-sustaining MS-MFCs for in situ coastal energy recovery and environmental monitoring.

Keywords: bioenergy; biomass; marine sediment; energy storage; energy conversion

Received: 4th Feb 2026; Revised: 16th June 2026; Accepted: 27th July 2026; Available online: 9th August 2026

1. Introduction

Sediment microbial fuel cells (S-MFCs) are bioelectrochemical devices that leverage the metabolism of electroactive microorganisms to convert organic substrates naturally present in sediments into electrical energy (Yang & Chen, 2021). Their operation intrinsically couples biochemical reaction kinetics with charge transport, mass transfer, and interfacial phenomena, core concerns in chemical reaction engineering and electrochemical process analysis. In S-MFCs, bacteria conduct extracellular electron transfer (EET) to an anode embedded in the sediment matrix, enabling energy recovery from renewable organic matter in aquatic environments such as rivers, lakes, and coastal regions. Because these systems operate under ambient conditions without external power input, they offer low operating costs and minimal environmental impact (De Schamphelaire *et al.*, 2008; Hubenova *et al.*, 2024). From a transport perspective, the sediment acts as a heterogeneous porous medium where solid–liquid interfaces, diffusion constraints, and electrochemical boundary conditions strongly influence overall performance. These features make S-MFCs attractive for powering remote environmental sensors, low-power electronics, and in-situ monitoring platforms where conventional energy infrastructure is unavailable (Algar *et al.*, 2020).

Despite these advantages, S-MFCs commonly exhibit low power density due to slow electron transfer kinetics and high resistance at the biofilm–electrode interface (Mitov *et al.*, 2015). Such constraints reflect coupled kinetic and transport limitations resembling mixed-control regimes typical in electrochemical systems. Additional losses arise from mass-transfer barriers within the heterogeneous sediment and the complex architecture of biofilms, which hinder substrate

* Corresponding author
Email: marcelinus@live.undip.ac.id; marcelinus@lecturer.undip.ac.id (M. Christwardana)

https://doi.org/10.61435/ijred.2026.62325
ISSN: 2252-4940/© 2026.The Author(s). Published by CBIORE

diffusion and metabolite removal (Lee *et al*., 2015). These diffusion–reaction interactions underscore the importance of effective diffusivity, tortuosity, and accessible interfacial area in porous-media models. Performance can also be destabilized by temporal biofilm variability and the slow kinetics of redox mediators, producing fluctuating currents (Abazarian *et al*., 2023). Collectively, these factors impede large-scale and sustained deployment.

Marine sediment microbial fuel cells (MS-MFCs) represent a specific class of S-MFCs that exploit the relatively high organic content and strong intrinsic redox gradients found in coastal sediments (Zhou *et al*., 2018). Vertical redox stratification in marine sediments creates natural electrochemical gradients analogous to spatially distributed electrode potentials in layered systems. Beyond benthic energy harvesting, MS-MFCs may be integrated with plant-microbial fuel cells (PMFCs), particularly in mangrove ecosystems rich in root exudates and sedimentary organic matter, to provide an in-situ power supply for continuous coastal monitoring. However, operational stability remains sensitive to salinity shifts, tidal dynamics, and oxygen intrusion into sediments (Rahimnejad, 2023), highlighting the need for a systems-level approach that simultaneously accounts for biological production, charge transfer, and hydrodynamic boundary conditions.

Hydrochar (HC) has attracted attention as an electrode modifier in MS-MFCs because its high surface area and oxygen-containing functional groups (e.g., hydroxyl and carboxyl) can improve microbial adhesion and facilitate electron transfer at the biofilm–electrode interface (Christwardana *et al*., 2025). At the microscale, HC provides additional electrochemically active sites, effectively increasing interfacial area and modifying local charge-transfer resistance. These surface functionalities support biofilm formation and accelerate redox processes, thereby enhancing charge transfer (Delgado *et al*., 2024). Although HC is less conductive than activated carbon, its pseudocapacitive behavior can provide transient charge storage that stabilizes current output. HC is also sustainable and cost-effective because it can be produced from renewable biomass (Padhye *et al*., 2022), making it a promising material that integrates surface activity, short-term charge buffering, and environmental compatibility.

Acetate is a key substrate that electroactive microbial communities readily metabolize in sedimentary systems, yet its availability is often limited in natural environments (Ojha *et al*., 2025). Acetate concentration directly affects microbial reaction rates and electron flux, functioning similarly to a controllable reactant feed in bioelectrochemical systems. Supplementation can intensify microbial metabolism, increase electron delivery to the anode, and improve electrochemical performance (Gong *et al*., 2022). This substrate-driven modulation simultaneously influences biochemical kinetics and the electrochemical current response, reinforcing the tight coupling between reaction-rate control and charge transport. However, the combined effects of acetate addition and HC-based electrode modification on S-MFCs have not been comprehensively examined, particularly in ways that connect electron transfer efficiency with capacitive behavior under realistic sediment conditions.

In this context, bidirectional modulation in MS-MFCs refers to the simultaneous tuning of electron transfer kinetics and capacitive energy storage through both electrode material properties and substrate availability (Caizán-Juanarena *et al*., 2020). This dual control reflects a hybrid conversion–storage system in which faradaic and non-faradaic processes coexist and interact dynamically. While earlier studies often prioritized current-density enhancement, emerging work emphasizes capacitive contributions to sustaining steadier energy output (Lee *et al*., 2015), which can be interpreted using transient electrochemical models that incorporate both kinetic and capacitive elements.

Mangrove sediments, rich in organic matter and electroactive microorganisms, offer a particularly suitable natural setting for microbial fuel cell implementation (Nagarajan *et al*., 2025). They function as naturally occurring bioreactors where reaction kinetics, transport limitations, and electrochemical gradients coexist within a confined porous matrix. Coupling MS-MFCs with mangrove plants (i.e., PMFC concepts) could further support self-sustaining power generation via rhizosphere-driven substrate supply. Yet, the mechanistic relationship between pseudocapacitive electrode behavior and microbial electron transfer kinetics remains insufficiently resolved in real sediment environments, limiting the development of predictive models that link material properties, reaction kinetics, and macroscopic performance. Many prior studies have evaluated charge storage and bioelectrocatalytic activity separately, overlooking their interdependence in determining current stability and energy storage capacity. Moreover, the synergistic impact of HC modification and acetate supplementation on bidirectional energy regulation has not been quantitatively established.

Accordingly, this study investigates the combined effects of hydrochar and acetate on bidirectional regulation of electron transport and capacitive behavior in MS-MFCs. Its innovation lies in developing a mechanistic framework that directly correlates pseudocapacitive charge storage with microbial electron transport in marine sediment systems, enabling translation from laboratory observations toward scalable process design. The work systematically quantifies bi-modal energy modulation induced by HC and acetate by integrating electrochemical kinetics, capacitive analysis, and sediment redox characterization. A structured evaluation of key redox and transport-relevant parameters (pH, ORP, conductivity, and TDS) provides a mechanistic basis for improving MS-MFC performance and supports progress toward mangrove-based PMFCs for sustainable coastal energy applications.

2. Materials and Method

2.1 Bioelectrochemical Design and Preparation

Three identical bioelectrochemical system (BES) reactors using a flat-plate design were fabricated from clear acrylic glass. Each reactor had an anode compartment isolated from the cathode by a Nafion 117 cation exchange membrane (Dupont, USA). The anode chamber has a total capacity of 28 mL, including 25 mL of anolyte solution, thereby providing 3 mL of air space for gas exchange (Liu & Logan, 2004). The anolyte used was Hoagland plant development medium supplemented with ammonium bicarbonate (2.5 g L^{-1}) as a nitrogen and inorganic carbon source, along with a phosphate buffer (pH 7.2). Nitrate and sulfate constituents were eliminated to mitigate undesirable redox interference while preserving microbial proliferation (Helder *et al*., 2012). The schematic of MFC reactor can be shown in Figure 1.

The anode and cathode electrodes used graphite carbon cloth with an active surface area of 7 cm^2. Copper wires with a diameter of 1 mm were firmly affixed to the electrodes and sealed with waterproof adhesive to provide a robust electrical connection. The cathode functions as an air-breathing electrode, with the electrolyte surface directly exposed to air, enabling oxygen to serve as the terminal electron acceptor without requiring additional aeration or circulation. This research used four anode compositions: (1) pure marine sediment, (2) marine sediment mixed with 5% (v/v) hydrochar, (3) marine sediment mixed with 10% (v/v) hydrochar, and (4)

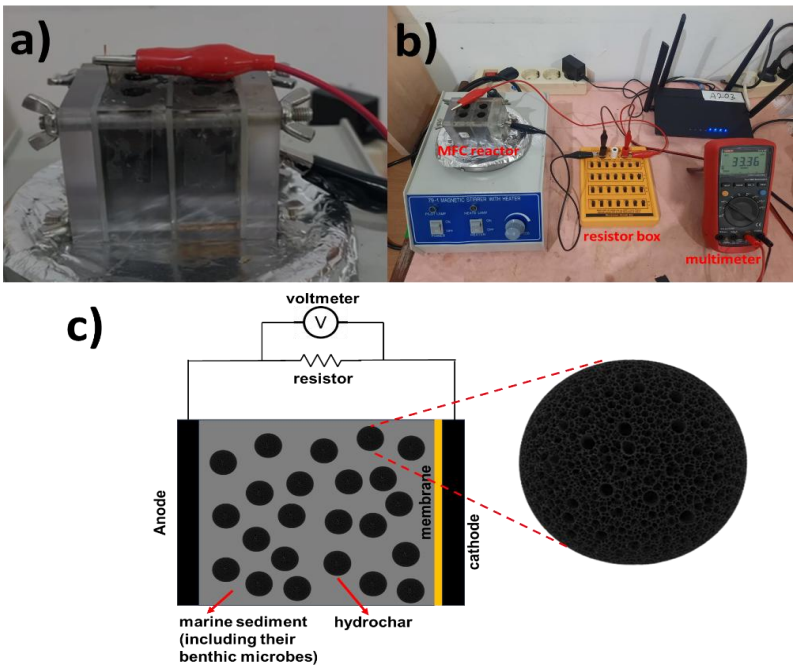

Fig. 1 a) Close-up of the lab-scale SM-MFC reactor, while b) Full measurement arrangement of SM-MFC reactor with resistor box and multimeter with data logger for long-term incubation measurement and c) their schematic diagram

marine sediment mixed with 15% (v/v) hydrochar. The hydrochar used in this study was derived from mango tree branch biomass, and its physical, chemical, and electrochemical characteristics have been reported in a previous study (Christwardana *et al*., 2025). The sediment sample was obtained from the coastal mangrove region of Tambak Lorok, Semarang City, Central Java, Indonesia (5°1.4467′ N, 4°0.9314′ E). All silt was homogenized, sieved to less than 1 mm, and kept at 4°C prior to use.

2.2 BES Reactor Operation

2.2.1 Electricity Production Experiment (MFC Mode)

From day one to day thirty, all BES reactors functioned in power-generation mode. The anode and cathode were linked with an external resistor of 1000 Ω to ensure uninterrupted electron flow (Tang *et al*., 2025). On day 21, 1 M sodium acetate (NaAc) was used as an external carbon source to promote microbial metabolism and increase current production (Luo *et al*., 2016). The reactors were preserved in a climate-controlled environment (27–30 °C, 80% relative humidity) with a 12:12 h light–dark cycle to replicate natural settings.

2.2.2 Electricity Storage (Capacitive Mode)

Electrical storage capacity testing was performed on days 0, 7, 14, 21, and 30 using cyclic voltammetry (CV) analysis to assess the capacitive characteristics of marine sediment with and without hydrochar supplementation. To prevent disturbance of the anode biofilm during prolonged operation, all cyclic voltammetry measurements were performed ex situ using a three-electrode setup including a glassy carbon working electrode, an Ag/AgCl reference electrode, and a stainless-steel counter electrode. Each experiment used a novel sediment-hydrochar amalgamation that was not electrically linked to the primary MFC. The specific capacitance (C_{sp}) was derived from the area of the CV curve using the following equation (Sharma & Chand, 2023):

$$C_{sp} = m.k.(V_2 - V_1).A \quad (1)$$

A represents the area of the CV curve, m denotes the mass of the active electrode (g), k signifies the potential scan rate (mV/s), while V_2 and V_1 indicate the top and lower bounds of the potential window, respectively.

2.2.3 Measurement and Analysis

Cell voltage was manually recorded using a digital multimeter (UNI-T 61E) throughout the reactor's operational duration. An Arduino-based potentiostat was used for electrochemical investigation by cyclic voltammetry to evaluate the charge storage capacity of electrodes derived from marine sediment. Liquid samples were collected every 7–9 days using sterile syringes fitted with microfilters to avert contamination by solid particles, thereafter kept at 4°C prior to further analysis. Physicochemical parameters, including conductivity, pH, and oxidation-reduction potential (ORP), were assessed using a portable 4-in-1 water meter (CQQ-L123). The acquired data were used to analyze the bioelectrochemical performance and assess the energy conversion and storage efficiency of the SM-MFC system.

2.3 Statistical Analysis

Each measurement was conducted in three independent replicates, and the data are expressed as mean ± standard deviation.

3. Results and Discussion

3.1. Electrochemical Characterization

3.1.1. Redox Behavior

The cyclic voltammetry (CV) curves of MS-MFCs with different hydrochar (HC) concentrations (0–15%) illustrate the development of redox behavior influenced by biofilm proliferation and electrode modification (Figure 2a-d),

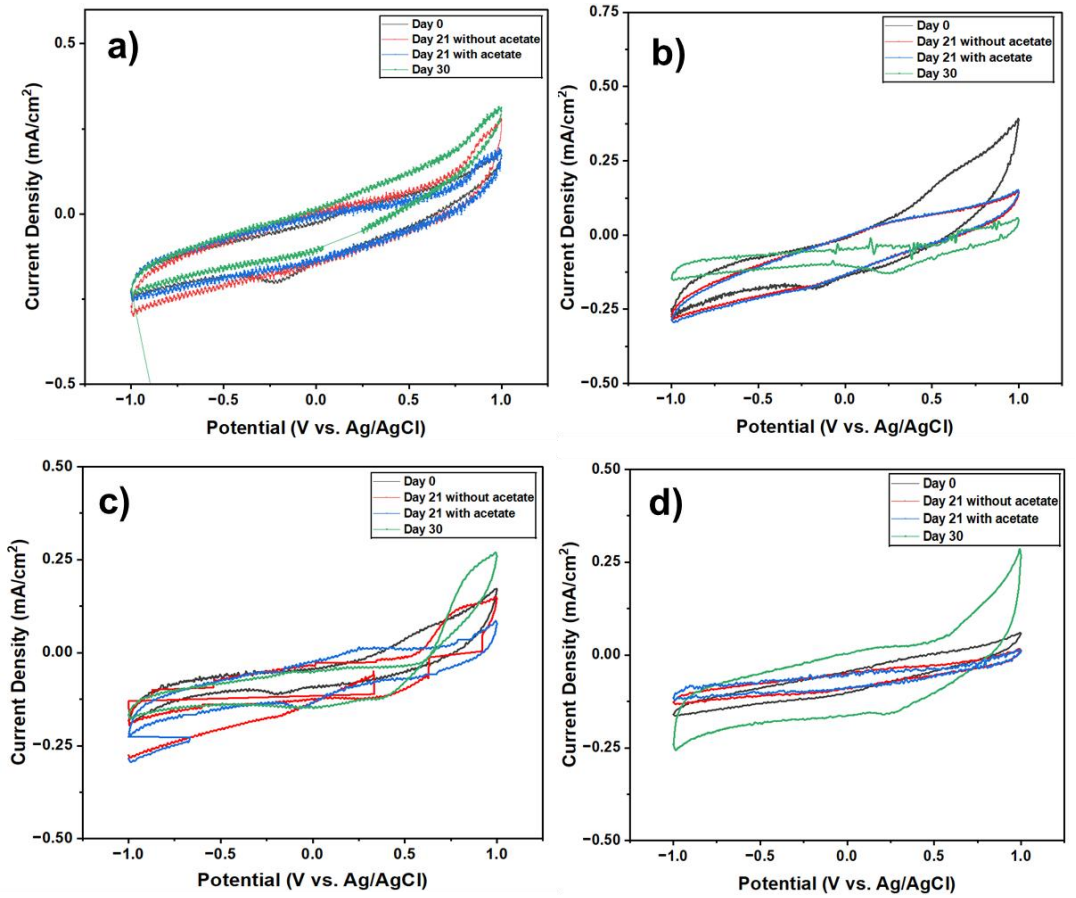

Fig 2. CV spectra MS-MFCs using a) MS, b) MS+5%HC, c) MS+10%HC, and d) MS+15%HC at day 0, day 21 (without acetate), 21 (with acetate), and 30.

consistent with the use of CV for evaluating extracellular electron transfer and electroactive microbial biofilms in bioelectrochemical systems (Harnisch & Freguia, 2012; Babauta *et al*., 2012). The CV response illustrates the cumulative impacts of interfacial charge transfer, ion transport in porous electrodes, and temporal biofilm development, which are essential parameters in the investigation of electrochemical systems (Marsili *et al*., 2010). On day 0, all electrodes exhibited a characteristic capacitive electric double-layer profile, indicating the lack of electroactive species. This trend signifies predominant non-faradaic charge storage, often seen in carbon-based electrodes before biological activation (Elgrishi *et al*., 2018). After 21 days, a faint redox signal emerged, indicating microbial colonization and the activation of certain redox sites. The progressive emergence of redox peaks indicates the initiation of kinetically regulated electron transfer mechanisms facilitated by microbial redox proteins. The incorporation of acetate increased both anodic and cathodic currents, reduced the peak potential difference (ΔEp), and displaced the oxidation peak towards the positive, together signifying improved bioelectrocatalytic oxidation and expedited electron transport. This peak development indicates a shift from diffusion-limited to mixed kinetic-capacitive control in the electrode-biofilm system. On day 30, a distinct redox peak signified the establishment of an electroactive biofilm and an effective charge transfer channel between the microorganisms and the electrode. The stable redox behavior signifies the establishment of a mature bioelectrochemical interface with improved electron flow continuity.

The HC content significantly influences redox reversibility. Variations in hydrochar loading influence electrode porosity, effective surface area, and local charge distribution, which together determine electrochemical reversibility. Moderate enhancements (5–10%) improved the current responsiveness and peak symmetry by using the synergy between capacitive and faradaic mechanisms. This synergy demonstrates the simultaneous involvement of pseudocapacitive charge storage and faradaic electron transport, which is pertinent to enhancing transient electrochemical performance (Mathis *et al*., 2019). The 10% HC electrode demonstrated quasi-reversible behavior, indicating efficient microbe-electrode interaction via cytochrome c and flavins. The quasi-reversible kinetics indicate less interfacial resistance and enhanced electrical coupling between microbial redox centers and the carbon surface (Zhu *et al*., 2022; Delgado *et al*., 2024). At 15% HC, the initial resistance caused by diminished porosity was surmounted by the development of a conductive biofilm, yielding the maximum current. The finding underscores the interplay between structural transport constraints and physiologically mediated conductivity augmentation (Fan *et al*., 2021). Hydrochar improved electron mobility and redox coupling in the biofilm, with 15% HC demonstrating promising preliminary outcomes for extracellular electron transfer efficiency (Delgado *et al*., 2024).

3.1.2. Rate-Determining Step (RDS) Analysis

Determining whether charge transfer in MS-MFCs is governed by diffusion or surface kinetics is essential for enhancing electron transport and ensuring long-term stability. This difference pertains directly to finding the rate-limiting phase in coupled bioelectrochemical reaction-transport systems. Cyclic voltammetry (CV) was conducted at scan rates ranging from 100 to 1600 mV s^{-1} to ascertain the rate-determining step (RDS) (Figures S1–S4). Scan-rate-dependent cyclic voltammetry

analysis offers a diagnostic framework often used to differentiate kinetic control from mass transport limitations in electrochemical systems. All electrodes exhibited a comparable linear relationship between scan rate and current density (Figures S5–S8), indicating uniform electrochemical behavior throughout operation. This consistency indicates a repeatable electrode design and consistent interfacial conditions throughout the evaluated combinations.

On day 0, the anode devoid of biofilm displayed little faradaic activity, with peak current precisely proportional to scan rate ($i_p \propto v$), therefore validating a surface-controlled mechanism via double-layer charging and adsorption of residual redox species. This demonstrates the inactivity of microbial catalysis and indicates that the electrode surface serves as the principal locus for initial electron transfer. The observed behavior corresponds to a non-diffusive, interfacial charge storage regime. Following 21 days of operation devoid of acetate, the biofilm commenced growth; nevertheless, the faradaic response remained feeble, continuing to display a I_p and v correlation. This signifies that electron transfer remains constrained by interfacial processes, such sluggish redox reactions inside the biofilm or capacitive effects, rather than by mass diffusion from the bulk media.

After the introduction of acetate on day 21, the faradaic current exhibited a pronounced rise, characterized by a sublinear correlation ($I_p \propto v^{0.5}$), suggesting a transition to diffusion-limited kinetics as per the Randles–Ševčík equation (Suliborska *et al*., 2019). The shift indicates that reaction rates exceed substrate transport rates within the biofilm matrix. Elevated microbial activity and the suppression of acetate diffusion across the metabolic layer render mass transport the principal limiting factor. By day 30, the system reached an advanced phase characterized by a denser, more resistant biofilm and almost exhausted acetate levels. The electrochemical response is diffusion-limited due to the restricted mobility of residual substrate inside the thick biofilm matrix, which hinders electron transmission (Taherzadeh *et al*., 2012). The phenomenon of diffusion control is typical of transport-limited porous electrochemical systems. This behavior aligns with a mature SMFC, whereby biofilm proliferation and substrate decomposition augment transport resistance (Rafiee *et al*., 2024).

The slope of the current density to scan rate curve transitions from around 1.0 (days 3–9) to 0.5 (days 14–30), indicating a shift from surface-limited to diffusion-limited kinetics. The change from kinetic to transport control regimes is quantitatively represented by this progression. This time development demonstrates how biofilm thickening and acetate metabolism gradually transfer control of electron transfer from the interface to the mass transport barrier.

3.1.3. Kinetic Constants (ks) and Microbial Affinity

The electron transfer rate constant (k_s), derived from Laviron analysis, signifies the inherent kinetics of the interaction between the biofilm and the electrode (Christwardana *et al*., 2024). The parameter ks quantifies the heterogeneous electron transport kinetics at the biofilm–electrode interface. Figures S9–S12 and Table 1 illustrate the variations in ks corresponding to various hydrocar (HC) concentrations and operational durations. Kinetic descriptors are essential for comparing interfacial reaction rates across electrode designs. Theoretically, k_s is a positive kinetic parameter with no universal absolute minimum or maximum, where $k_s \rightarrow 0$ represents extremely sluggish electron transfer and higher k_s values represent faster heterogeneous electron exchange. However, the practically measurable k_s range in Laviron analysis is governed by the CV scan-rate window, peak separation, peak resolution, ohmic contribution, and the quasi-reversible validity domain of the model (Laviron, 1979; Eckermann *et al*., 2010; Pilz & Kielb, 2023).

On day 0, all samples had low k_s values (0.44–1.67 s^{-1}), indicating the absence of an electroactive biofilm. This regime exemplifies an interfacial system characterized by sluggish electron exchange rather than catalytic bioactivity. On day 21 (prior to acetate addition), k_s elevated in the majority of systems, specifically reaching 1.56 s^{-1} for MS and 2.10 s^{-1} for 15% HC, signifying the initiation of electron transport pathways. The rise in k_s signifies the gradual activation of charge transfer sites mediated by biofilms. Following the addition of acetate, a substrate-dependent impact was observed: HC15% exhibited a considerable increase (2.10 to 2.62 s^{-1}), but MS and HC5% shown decreases (1.56 to 1.03 and 1.85 to 0.78 s^{-1}), suggesting that the conductive matrix more efficiently channels acetate metabolism towards electroactive processes. The observed decrease in k_s for HC5% following acetate addition is attributed to insufficient conductive pathways and a limited number of redox-active sites at low HC loading. Although acetate enhanced microbial metabolism, the 5% HC matrix was unable to accommodate the increased electron flux. This limitation resulted in local proton accumulation, pH fluctuations, increased thickness of extracellular polymeric substances (EPS) or biofilm formation, and elevated interfacial or mass-transfer resistance. In contrast, 10–15% HC provided a more continuous conductive network and greater redox-buffering capacity, which enabled more efficient transfer of acetate-derived electrons to the electrode. This difference emphasizes the impact of electrode conductivity in steering metabolic flux towards interfacial electron transfer. On day 30, the electrode with elevated HC concentration exhibited superior kinetic

Table 1
k_s of MS-MFCs using various HC concentration at day 0, day 21 (without acetate), 21 (with acetate), and 30

Sample	k_s (s^{-1})			
	Day 0	Day 21 before acetate addition	Day 21 after acetate addition	Day 30
MS	0.44 ± 0.002	1.56 ± 0.016	1.03 ± 0.020	1.77 ± 0.003
MS-HC5%	0.82 ± 0.003	1.85 ± 0.002	0.78 ± 0.009	0.91 ± 0.001
MS-HC10%	1.67 ± 0.028	1.59 ± 0.001	1.47 ± 0.002	3.19 ± 0.017
MS-HC15%	1.28 ± 0.001	2.10 ± 0.056	2.62 ± 0.013	3.49 ± 0.025

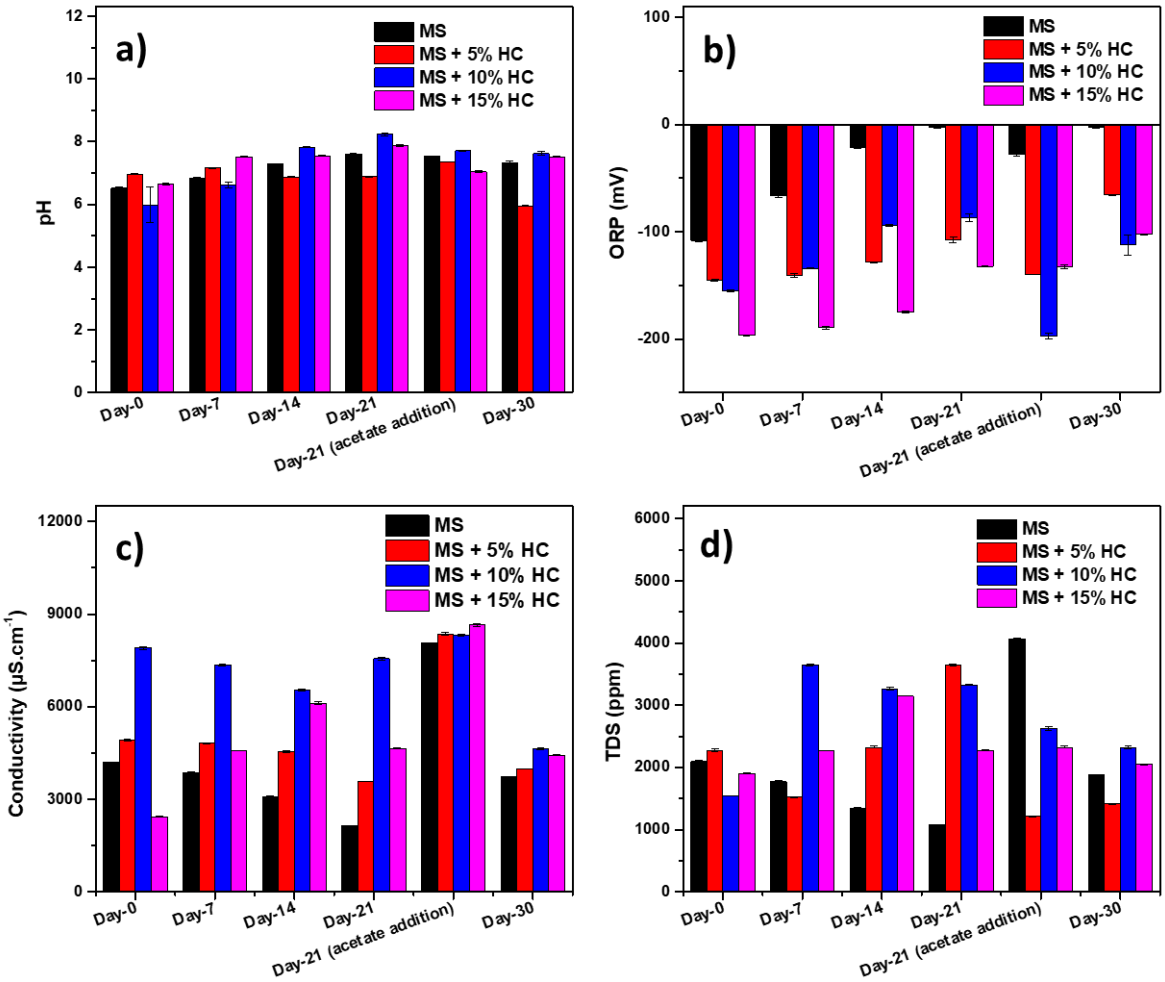

Fig 3. a) pH, b) ORP, c) Conductivity, and d) TDS of MS-MFCs using various HC concentration at day 0, day 21 (without acetate), 21 (with acetate), and 30.

performance, with k_s values of 3.49 s^{-1} (HC15%) and 3.19 s^{-1} (HC10%), in contrast to 1.77 s^{-1} (MS) and 0.91 s^{-1} (HC5%). These results indicate decreased kinetic barriers for electron transport at higher HC loadings. In this study, HC15% produced the highest day-30 k_s value (3.49 s^{-1}), indicating the kinetic optimum. However, HC10% reached 91.4% of this maximum (3.19 s^{-1}), suggesting that HC10% may represent a practical optimum when material efficiency and potential mass-transfer limitations are considered. The persistent rise in HC10–15% validates the dual function of HC as a conductive matrix and a substrate for biofilm support, ensuring prolonged electron transfer stability (Y. Xu *et al*., 2020). Conversely, a modest HC dosage (5%) was inadequate for enhancing conductivity and may have diminished the sediment's inherent charge-conducting channels (Han *et al*., 2025).

The significant association between k_s and HC concentration underscores the role of graphitic and redox-active groups in HC, which enhance electron mobility and augment microbial affinity for the electrode. This structure-kinetics connection connects the physicochemical qualities of materials to the rates of interfacial reactions. The temporary reduction in k_s in the HC-free system after acetate addition indicates that the non-conductive matrix cannot sustain effective biofilm-electrode communication. Conversely, the 15% HC-rich system exhibited steady kinetics, demonstrating that the conductive environment not only enhances electron transfer but also mitigates metabolic oscillations, leading to improved bioelectrochemical performance (Matsuzaki *et al*., 2024). transport barrier.

3.1.4. Local Electrochemical Environment: pH, ORP, Electroconductivity, and Total Dissolved Solid Analysis

The stability of anolyte pH is a crucial determinant affecting microbial activity, proton transport, and electron transfer efficiency in MS-MFC. The pH directly regulates proton availability and interfacial charge equilibrium in bioelectrochemical systems. Figure 3a illustrates the trajectory of pH changes. The control system (unmodified MS) exhibited a notable pH decline from 6.75 to 6.2 on day 7, indicating proton buildup in the absence of a functional buffering system. The incorporation of HC (5–15%) effectively mitigated this decline and maintained the pH within the range of 6.5–6.7. Such stabilization reduces proton buildup at the anode–biofilm contact, thereby reducing kinetic barriers for electron transmission. The buffering effect arises from the redox-active functional groups in HC, including quinones and phenolics, which facilitate proton absorption and improve proton–electron coupling (Delgado *et al*., 2024). By day 21, the system containing 10–15% HC had achieved a stable pH of 6.75–6.8, signifying equilibrium between proton generation and use. This equilibrium may indicate a steady-state balance between metabolic proton generation and electrochemical consumption. Following the introduction of acetate, both systems saw a

temporary decline in pH; yet, the reduction was less pronounced in MS+HC15% (6.35–6.6) relative to MS (6.1). This validates the function of HC as proton buffers, preserving acetate oxidation activity without inducing acidification (Matsuzaki *et al*., 2024). By day 30, the pH of HC had reverted to about neutral (6.55–6.75), signifying sustained buffering ability and enhanced microbial resilience.

The anolyte redox potential (ORP) indicates the electron-accepting capability and respiratory efficiency of microorganisms (Figure 3b). ORP acts as a macroscopic indication of the thermodynamic impetus for anaerobic electron transport. A lower ORP indicates more reductive circumstances, promoting electrogenic anaerobic respiration. On day 1, the MS ORP measured –200 mV; however, the introduction of HC decreased the baseline to –210 to –230 mV, suggesting that HC facilitate the establishment of a reductive environment via the labile carbon fraction and redox-active groups (T. Sun *et al*., 2017). During the first week, reductive circumstances escalated swiftly, particularly at 10–15% HC (–240 to –260 mV), signifying enhanced microbial colonization (Gupta *et al*., 2021). This shift signifies enhanced electron sink accessibility at the anode surface. On day 21, the ORP disparity between the MS and HC-treated systems reached 40–50 mV, substantiating the function of HC in enhancing the electrochemical gradient to expedite electron transport. Following the introduction of acetate, the ORP exhibited a significant decline, with MS+HC15% reaching –280 mV, indicating heightened activity within the electrogenic population. On day 30, the ORP was consistently more negative (–235 to –255 mV) compared to MS (–220 mV), indicating prolonged reductive stability (Wang *et al*., 2022). A prolonged low ORP signifies sustained reaction-transport coupling within the sediment matrix.

The electrical conductivity (EC) of the anolyte indicates the ion-conducting ability of the medium and is directly correlated with the internal resistance and cell efficiency (Figure 3c). EC indicates the efficiency of ionic transport, a significant factor in ohmic losses inside electrochemical systems. Initially, MS exhibited an electrical conductivity of 3.2 mS/cm, but the system with HC showed reduced values (2.0–3.2 mS/cm) attributable to the adsorption of free ions onto the HC surface. On day 7, the electrical conductivity (EC) rose markedly owing to microbial metabolic activity: MS+5%HC peaked at 6.0 mS/cm, while 10–15% HC maintained a more consistent range of 4.7–4.9 mS/cm. Regulated electrochemical evolution signifies restrained ion release and movement inside the porous sediment–electrode matrix. The elevated values at 5% HC indicate fast ion release, however may also augment internal resistance owing to excessive ion buildup. In contrast, 10–15% HC established an electrolyte equilibrium that decreased polarization losses. Following the introduction of acetate, all systems exhibited an elevation in electrical conductivity (6.0–6.3 mS/cm), with 15% HC attaining the peak values, indicating an enhancement of the microbial–electrolyte interaction amid vigorous metabolism (Huang *et al*., 2024). By day 30, the system stabilized within a range of 3.5–3.7 mS/cm, signifying a balanced electrochemical condition after acetate consumption. HC function as mild conductors and electrochemical buffers, stabilizing ion mobility and facilitating charge transfer (Delgado *et al*., 2024; Yang *et al*., 2016).

Total dissolved solids (TDS) indicate the concentration of dissolved ions resulting from microbial respiration (Figure 3d). TDS offers a comprehensive assessment of ionic production, movement, and adsorption in the anolyte. MS exhibited a greater TDS concentration (1,050 mg/L) compared to the system containing HC (900–1,000 mg/L), suggesting ion adsorption by the porous HC matrix. By day 7, total dissolved solids (TDS) escalated as a result of heightened metabolism, in the following order: MS+5%HC > MS+10%HC > MS+15%HC > MS. The ionic charge attained stability on day 14 (1,200–1,420 mg/L), signifying an equilibrium among ion release, absorption, and adsorption (Marzban *et al*., 2024). This equilibrium represents the dynamic ion balance characteristic of steady-state electrochemical systems. Following the addition of acetate, all systems exhibited a TDS surge (1,700–1,800 mg/L), but HC mitigated the significant escalation. By day 30, TDS readings fell to 1,100–1,200 mg/L, signifying a restoration of electrolyte conditions. The HC adsorption process mitigates ionic oscillations during periods of high activity and enhances recovery after metabolic stress (Ji *et al*., 2024).

The comprehensive investigation of pH, ORP, EC, and TDS validated the influence of HC in creating a stable electrochemical microenvironment in MS-MFCs. The combined parameters together delineate the reaction-transport regime that regulates bioelectrochemical performance. Based on the observed trends, EC/TDS and ORP were the parameters most affected by HC addition, whereas acetate addition mainly influenced ORP and pH due to the stimulation of microbial metabolism and substrate oxidation. Systems containing 10–15% HC demonstrate a significant negative connection between pH and ORP (neutral pH, ORP –250 to –265 mV), signifying ideal anaerobic conditions for electrogenic respiration (Q. Xu *et al*., 2023; Yan *et al*., 2024). The stability of pH and redox conditions improves EET, while the rise in EC and TDS signifies regulated ionic activity that reduces ohmic resistance without disturbing the electrochemical gradient. Among these parameters, EC is considered the most dominant factor in determining fuel cell performance because it directly affects ohmic resistance and therefore controls voltage and power generation. Higher EC reduces resistance, thereby minimizing voltage loss. This monitoring is crucial for sustaining steady-state functioning in electrochemical systems based on marine sediment. Acetate addition studies validate these findings, systems containing HC show less severe oscillations and expedited recovery. HC serve as dual-function materials: they are moderate conductors with significant redox capacity, ensuring chemical and biological stability to improve the efficiency and longevity of MS-MFCs (Dang *et al*., 2024; Delgado *et al*., 2024). From both technical and economic perspectives, the addition of HC is advantageous because it stabilizes redox conditions and enhances ionic conductivity without necessitating substantial external electrolyte supplementation. While pH and ORP are critical for sustaining electrogenic microbial activity, EC contributes most directly to power generation by reducing internal resistance. TDS serves as a supplementary indicator of ionic availability.

3.2. Energy Storage Characterization

The capacitive characteristics of MS-MFC serve as a crucial metric for evaluating the system's capacity to store and discharge charge during electrochemical processes. Capacitance represents the transitory equilibrium among ionic transport, interfacial charge buildup, and faradaic reactions in porous electrochemical systems. Assessing the capacitance of marine sediments, particularly after alteration with HC, is essential for enhancing charge storage and energy harvesting mechanisms. he expected energy-storage behavior is not completely constant during operation; rather, it fluctuates during early biofilm formation and substrate adaptation, then approaches a more stable condition after the establishment of mature electroactive biofilms. Energy-storage stability can be evaluated from capacitance retention and energy retention, indicating that stable capacitance and voltage are both essential

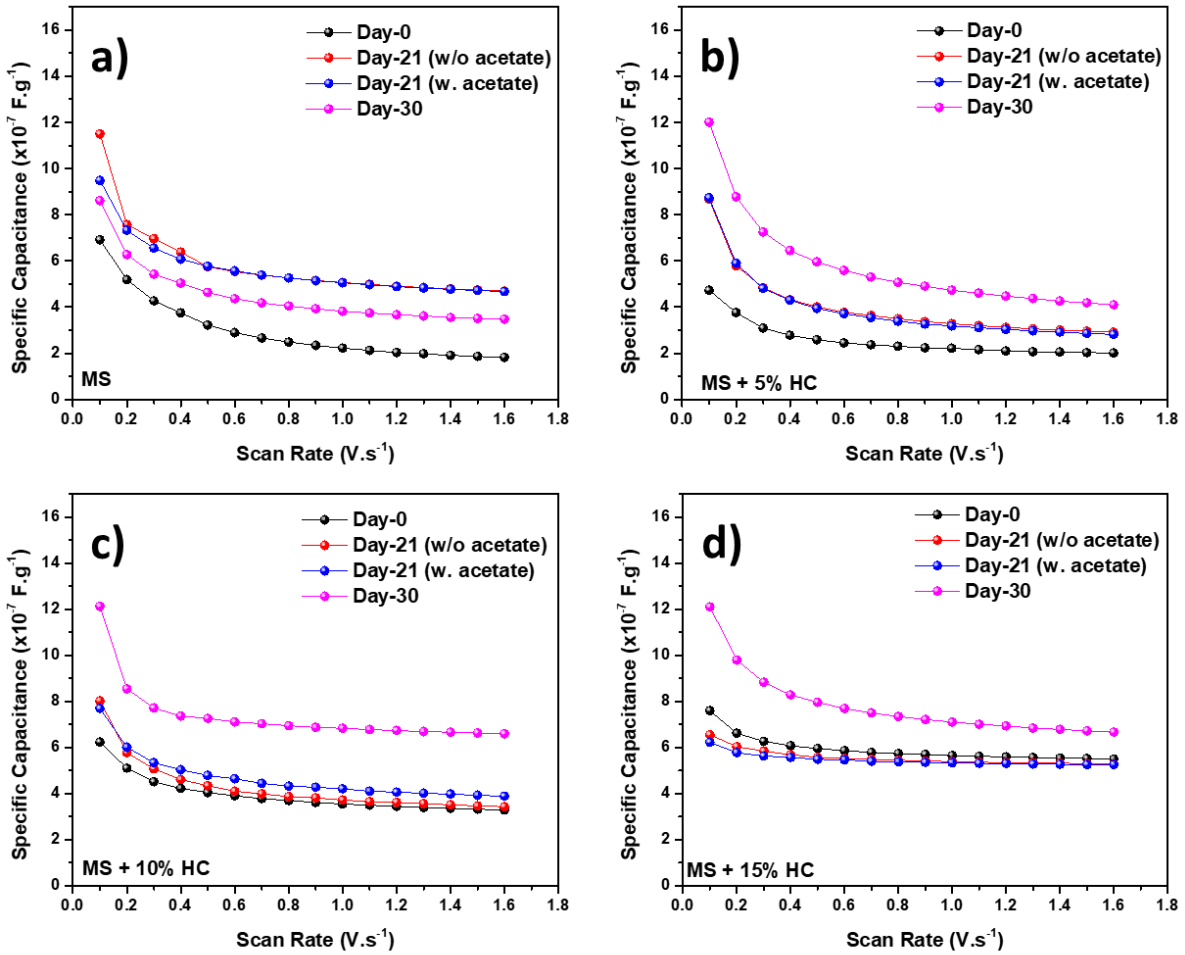

Fig 4. Specific capacitance of MS-MFCs using a) MS, b) MS+5%HC, c) MS+10%HC, and d) MS+15%HC at day 0, day 21 (without acetate), 21 (with acetate), and 30.

for maintaining reliable MS-MFC output. The reported capacitance in this study is interpreted as the apparent total capacitance, which encompasses the combined contributions of double-layer capacitance, hydrochar-derived pseudocapacitance, and biofilm-associated faradaic charge storage.

Figure 4a illustrates a progressive augmentation in MS capacitance. Day 0 has a reduced value due to little microbial activity. On day 21, in the absence of acetate, the capacitance exhibits a slight rise due to biofilm proliferation. The presence of acetate demonstrates a more pronounced rise, affirming that acetate acts as an auxiliary carbon source, augmenting the system's metabolism and electrochemical response. This behavior indicates a correlation between metabolic rate and capacitive charge buildup. On day 30, the capacitance exhibits a modest reduction, indicating the stability of the microbial population after a time of fast expansion. This slight reduction also indicates that energy storage tends to shift from rapid growth to a more stabilized charge-storage state after biofilm maturation. The almost rectangular CV profile and the linear connection between current and scan rate suggest the predominance of capacitive processes. Such patterns are indicative of systems governed by non-diffusion-limited charge storage. A redox peak at around ±0.25 V (vs. Ag/AgCl) is linked to the quinone/hydroquinone pair on the HC surface, which enhances pseudocapacitance. Charge storage arises from two mechanisms: (i) double-layer capacitance resulting from ion adsorption in carbon pores, and (ii) faradaic reactions involving functional oxygen groups. The interplay of these processes demonstrates the mixed capacitive–faradaic behavior characteristic of functionalized carbon electrodes. The integration of these two processes leads to enhanced capacitance as the biofilm develops. To clarify the contribution of each process, the day-0 capacitance was interpreted as primarily reflecting abiotic double-layer and hydrochar-associated pseudocapacitive behavior, given the minimal biofilm activity at this stage. The increase in capacitance from day 0 to day 21 was attributed to biofilm development, while the subsequent increase following acetate addition was ascribed to microbial metabolism-dependent faradaic electron transfer. The biofilm's contribution was determined by subtracting the day-0 capacitance from the day-21 capacitance measured prior to acetate addition. The effect of acetate was determined by subtracting the day-21 capacitance before acetate from the value obtained after acetate addition. Because microbial faradaic processes and hydrochar pseudocapacitance were not fully separated, the reported capacitance values represent combined electrochemical responses.

In MS + 5% HC (Figure 4b), capacitance exhibited a consistent increase until day 21, followed by a further rise with the introduction of acetate. Acetate augments microbial metabolism, leading to maximum capacitance on day 30 (Gu *et al.*, 2024). This pattern indicates that metabolic activity directly influences available charge storage sites. HC at this

concentration augment conductivity and electron transport, establishing an optimal milieu for sustained microbial proliferation (Heenen *et al.*, 2022; Zhang *et al.*, 2025). The observed increase through day 30 indicates that 5% HC facilitates progressive development of energy storage; however, the system may require an extended adaptation period to achieve stable capacitive behavior.

The pattern of capacitance increase was similar in MS + 10% HC (Figure 4c), although exhibited a more pronounced reaction to acetate. A notable escalation occurred from day 0 to day 21, after which capacitance development started to stabilize around day 30. This deceleration signifies that the microbial community is approaching a stable phase. Capacitance stabilization signifies the saturation of the electrochemically active surface area. HC at this concentration provide ideal conductive routes for electron transfer and promote the development of mature electrogenic biofilms (Han *et al.*, 2025). Therefore, 10% HC is favorable for stable energy storage, as it provides both enhanced capacitance and reduced fluctuation following biofilm maturation.

In MS + 15% HC (Figure 4d), capacitance exhibited a significant rise until day 21 and sustained high levels until day 30, particularly in the presence of acetate (Gu *et al.*, 2024; J. Sun *et al.*, 2023). The decelerating growth rate from day 21 to day 30 indicates possible nutritional or diffusion stress attributable to the elevated HC content. Such stress is compatible with transport constraints in adsorptive, very porous materials. Surplus HC may result in competition for pore space, excessive nutrient adsorption, or alteration of ionic gradients that impede microbial activity. The presence of acetate sustained a high capacitance response, confirming the synergy between acetate and HC in preserving electrogenic activity. While 15% HC offers a high charge-storage capacity, its stability is more susceptible to mass-transfer limitations. Consequently, achieving high capacitance requires balancing this with stable ion and substrate transport.

Increased HC concentrations led to persistent enhancements in capacitance, particularly when coupled with acetate. At low concentrations (5% HC), conditions conducive to microbial proliferation are swiftly created; however, at 10–15% HC, elevated conductivity and redox site density improve charge storage, albeit with the drawback of possible growth inhibition due to nutrient scarcity at higher concentrations (Feng *et al.*, 2022). This trade-off illustrates the equilibrium between surface functionality and mass transport limitations. These results indicate an optimal point, beyond which further increases in HC provide declining returns (Chen *et al.*, 2025). The stability of energy storage directly influences MS-MFC performance by maintaining consistent voltage, minimizing transient current fluctuations, and enhancing the reliability of charge and discharge processes during operation. Instability in capacitance or voltage results in unreliable stored energy and power output. Therefore, the optimal condition is not solely the achievement of maximum capacitance, but rather the attainment of high capacitance with stable retention over time. From this perspective, the addition of HC, particularly at 10–15%, enhances both technical performance and economic feasibility by improving charge storage without the need for additional external energy-storage components.

3.3. Energy Production Characterization

The control MS-MFC containing only marine sediment (MS, black) produced very low current densities (0.05–0.10 mA m^{-2}) throughout the first 21 days (Figure 5a). This weak output is consistent with a kinetically constrained system dominated by high interfacial resistance, where early biofilms exhibit elevated charge-transfer impedance and the sediment lacks readily biodegradable substrates, resulting in slow EET in the absence of effective natural mediators. Adding 5% hydrochar (HC, red) immediately shifted the response: current density rose rapidly within the first week to ~0.40–0.45 mA m^{-2} (days 5–7), ~3× higher than MS. This activation-controlled rise indicates improved interfacial conductivity and facilitated electron transport, supported by redox-active quinone/hydroquinone moieties and the pseudocapacitive carbon matrix that enables charge storage–discharge. However, by day 21 the current declined to ~0.15 mA m^{-2}, consistent with depletion of redox-labile fractions and slower biodegradation of more recalcitrant hydrochar components, implying a transition from kinetically favorable operation to transport- or substrate-limited control.

Among the pre-acetate systems, 10% HC (blue) showed the most stable performance, suggesting an optimal balance between conductive surface area and mass-transfer accessibility. After a brief early decline (microbial adaptation), current increased during days 13–15 to ~0.50 mA m^{-2} and then stabilized at ~0.35–0.40 mA m^{-2} through day 21, yielding the greatest cumulative electron flow. This steady regime reflects reduced charge-transfer resistance and sustained EET enabled by greater conductive area and redox-site density (Leng *et al.*,

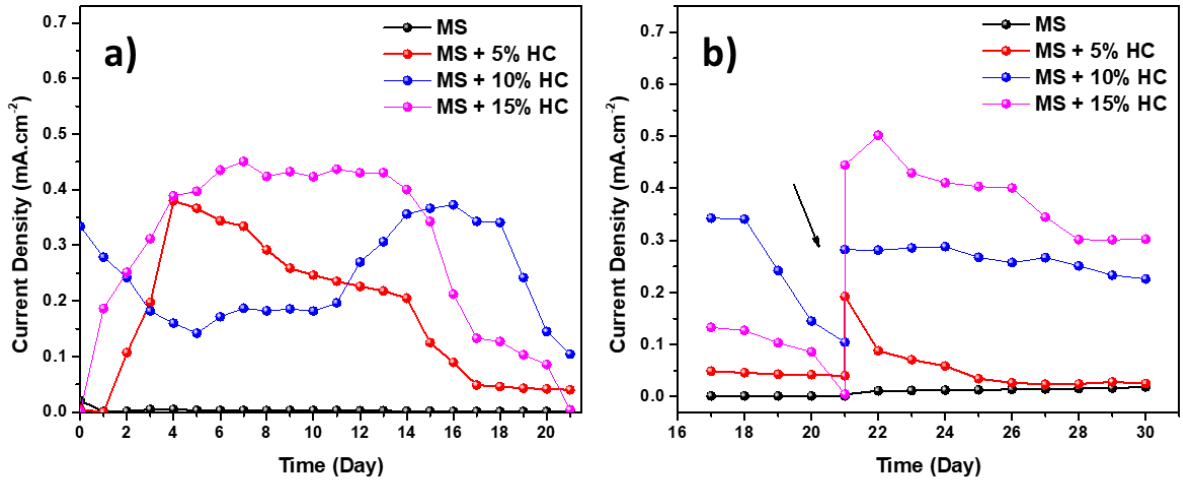

Fig 5. Current density of MS-MFCs using various HC concentration a) before and b) after acetate addition.

Table 2
Maximum Power Density of SM-MFCs over the time for 30 days of incubation

Sample	*MPD* (mW.m^{-2})					
	Day 0	Day 7	Day 14	Day 21 before acetate addition	Day 21 after acetate addition	Day 30
MS	0.023 ± 0.002	0.035 ± 0.004	0.046 ±0.002	0.001 ± 0.000	0.004 ± 0.001	0.043 ± 0.002
MS-HC5%	0.034 ± 0.003	13.114 ± 0.005	8.014 ± 0.003	0.207 ± 0.001	1.624 ± 0.005	0.062 ± 0.001
MS-HC10%	0.067 ± 0.001	18.748 ± 0.011	21.786 ± 0.013	0.468 ± 0.004	4.857 ± 0.003	0.081 ± 0.001
MS-HC15%	0.075 ± 0.003	20.763 ± 0.022	23.133 ± 0.034	2.589 ± 0.015	7.856 ± 0.027	1.173 ± 0.010

2021; Hou *et al*., 2010). In contrast, 15% HC (pink) exhibited a burst–decay pattern: a high peak (~0.55 mA m^{-2}, days 6–14) followed by a sharp decline to near-baseline by days 20–21, consistent with transient overactivation followed by diffusion or inhibitory constraints. At excessive HC loading, inhibitory effects (e.g., alkaline ash, soluble phenolics, or thicker biofilm accumulation) can increase diffusion resistance (Quintana-Najera *et al*., 2021). Although 15% HC demonstrates a strong initial electrochemical response, the observed pre-acetate burst–decay pattern indicates that this loading may lack stability for long-term field operation unless mass transfer, pH variation, and potential leaching of inhibitory organic compounds are effectively managed.

After acetate supplementation on day 21 (Figure 5b), all treatments increased in current, but the magnitude and persistence depended strongly on HC content, indicating a shift toward reaction-rate-controlled generation when substrate becomes available. The MS control (black) remained weak (<0.15 mA m^{-2}) and returned to baseline, supporting that acetate alone cannot overcome sediment structural resistance without a conductive amendment (Luo *et al*., 2016). With 5% HC (red), current increased to ~0.20–0.25 mA m^{-2} but decayed quickly, implying limited redox-site availability at low HC loading and incomplete conversion of metabolic flux into sustained charge transfer (Delgado *et al*., 2024; Dang *et al*., 2024; Wei *et al*., 2025). The 10% HC system (blue) responded more strongly and stably: current rose to ~0.45–0.50 mA m^{-2} on day 23 and persisted at ~0.30–0.35 mA m^{-2} until day 30, consistent with expanded conductive area, more redox groups, faster charge-transfer kinetics, and reduced polarization losses. The highest peak and long-term stability were observed with 15% HC (pink): current climbed to ~0.53 mA m^{-2} and sustained ~0.40–0.45 mA m^{-2} to day 30, indicating robust pseudocapacitive electron storage, a more continuous conductive microstructure, and substantial electrogenic biofilm colonization (Delgado *et al*., 2024; Mosali *et al*., 2025). Under sufficient acetate supply, the electrochemical advantages of high HC appear to outweigh or mitigate earlier inhibitory tendencies. However, the more pronounced pH decrease and reduced rate of capacitance growth following acetate addition suggest that 15% HC remains susceptible to acidification, excessive solid accumulation, pore obstruction, and biofilm thickening during extended operation. Therefore, 15% HC should be regarded as the most effective short-term treatment, rather than as a guaranteed sustainable long-term optimum.

On day 0, power densities were low but ordered by HC loading, MS+15%HC (0.075 mW m^{-2}) > MS+10%HC (0.067 mW m^{-2}) > MS+5%HC (0.034 mW m^{-2}) > MS (0.023 mW m^{-2}), demonstrating the direct role of conductive surface availability in activation-controlled power output. By day 7, HC-amended systems increased sharply to 13.114 mW m^{-2} (5% HC), 18.748 mW m^{-2} (10% HC), and 20.763 mW m^{-2} (15% HC), consistent with HC providing redox sites, conductivity, and porosity that accelerate biofilm colonization, strengthen EET, and enhance organic breakdown (Leng *et al*., 2021; Thunshirn *et al*., 2022). On day 14, higher HC loadings performed best, 21,786 mW m^{-2} (10% HC) and 23,133 mW m^{-2} (15% HC), suggesting greater carbon contribution from hydrochar, more adsorptive sites, and progressive release of organics sustaining microbial activity (Chen *et al*., 2025). MS and MS+5% HC decreased slightly from day 7 yet remained above day 0, indicating low-dose HC mainly accelerates early biofilm activation.

Approaching day 21 (pre-acetate), power density dropped across treatments, consistent with depletion of readily degradable substrates, accumulation of organic acids and protons, and pH suppression that inhibits microbial metabolism (Nourbakhsh *et al*., 2020; Puig *et al*., 2010), indicating a shift toward diffusion/mass-transfer constraints. Even so, 10% and 15% HC retained higher outputs (0.468 and 2.589 mW m^{-2}), implying better electrochemical buffering and structure. After acetate injection, performance rebounded—particularly for 10% HC (4.857 mW m^{-2}) and 15% HC (7.856 mW m^{-2})—because acetate restores substrate availability and directly feeds central metabolism (acetate → acetyl-CoA), increasing electron production and enriching acetate-utilizing electrogens (Mutyala & Kim, 2022). Hydrochar simultaneously acts as a conductive reservoir that supports biofilm stability and electron transport efficiency. By day 30, all systems declined again, consistent with nutrient limitation and prolonged "fatigue," including hydrochar pore blockage by biofilm and increased diffusion resistance (Teng *et al*., 2010). Nevertheless, MS+15%HC remained highest (1.173 mW m^{-2}), followed by MS+10%HC (0.081 mW m^{-2}), MS+5%HC (0.062 mW m^{-2}), and MS (0.0432 mW m^{-2}), indicating that 10–15% HC provides a more resilient electrochemical environment and sustained EET. This decline indicates that long-term sustainability should be assessed using multiple parameters, including peak power density, power retention, pH stability, capacitance retention, and resistance to diffusion limitation. Although the higher day-30 value of 15% HC demonstrates superior short-term resilience, the subsequent decline suggests caution when applying it in long-term systems.

Table 2 indicates an optimal HC window of ~10–15%, reaching peak power densities around ~23 mW m^{-2}. This range reflects a practical compromise: increasing conductivity and redox-site density with higher carbon loading, while avoiding excessive transport resistance. Although the absolute power remains modest for a small-scale, non-aerated reactor, the improvement represents an approximately 3–5× enhancement relative to conventional sediment-MFC performance under natural conditions. A 10% HC dosage is recommended for long-term field operation because it provides stable current generation and reduces the risks of diffusion limitation,

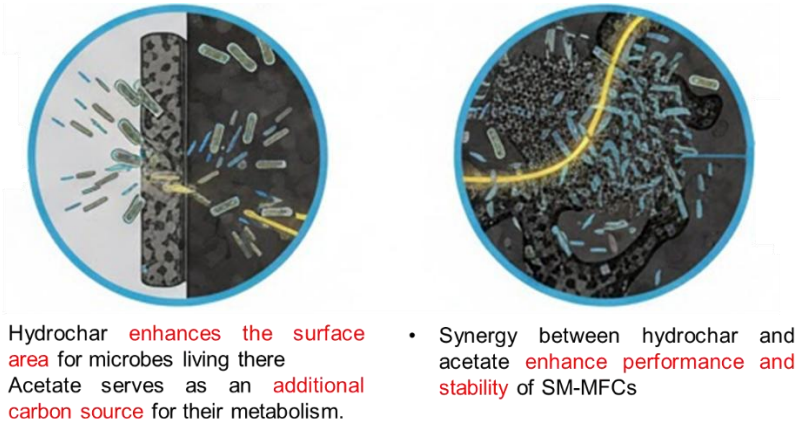

Fig 6. Schematic illustration of the synergistic roles of hydrochar and acetate in MS-MFCs.

excessive biofilm accumulation, soluble phenolic inhibition, and pH suppression. The 15% HC treatment defines the upper operational limit within the tested range and is appropriate when maximum short-term power output is necessary. However, this higher dosage requires careful monitoring of pH, ORP, EC, dissolved organic and phenolic compounds, and biofilm thickness. These findings demonstrate that 10–15% HC is the effective performance window, with 10% HC as the conservative choice for sustained use and 15% HC as the maximum loading that demands operational controls.

3.4. Synergistic Role of Hydrochar and Acetate in MS-MFCs

The investigation of current density, maximum power density, and capacitive behavior reveals a significant interrelation among HC content, microbial activity, and the electrochemical performance of MS-MFCs. These parameters jointly delineate the dynamic equilibrium between reaction kinetics and charge transport within the bioelectrochemical system. The incorporation of HC at elevated concentrations (10–15%) significantly augmented current density and power density, with a rise in capacitance indicative of biofilm proliferation and enhanced microbial metabolism. The rise of capacitance indicates a growth of the electrochemically accessible surface area and enhanced interfacial charge accommodation. The first current spike is propelled by elevated electron exchange transfer via redox-active groups and augmented surface area for microbial colonization, which directly improves power density (Christwardana *et al.*, 2024). This transitory reaction indicates a transition from activation-controlled to transport-facilitated electron transfer. As the biofilm stabilizes and substrate consumption advances, performance variations indicate changes in metabolic dynamics.

In systems supplemented with acetate, the enhancement of capacitance and power density is more significant due to acetate's facilitation of microbial catabolic activity, which amplifies electron flow and the production of redox mediators. The acetate-induced response exhibits substrate-limited behavior evolving into an acceleration of the reaction rate. The synergistic impact of pseudocapacitive HC and acetate leads to prolonged enhancements in power density and capacitance, indicating that HC functions as both a biofilm scaffold and a charge reservoir, hence promoting long-term EET stability (Chen *et al.*, 2025; Q. Xu *et al.*, 2023; Delgado *et al.*, 2024). This trend indicates enhanced temporal decoupling between microbial electron production and electrode charge acceptance. The dual function elucidates why elevated HC concentrations are ideal for the efficacy of MS-MFCs.

HC offers a conductive matrix that improves microbial adherence and increases the active surface area for electron transfer, while its pseudocapacitive characteristics facilitate temporal charge storage and release, hence stabilizing electron flow during metabolic variations (Wei *et al.*, 2025). This buffering alleviates variations in current density caused by temporary metabolic and mass-transfer limitations. Acetate facilitates this process by supplying an accessible carbon source, expediting microbial respiration, and improving EET, especially in electroactive species like Geobacter and Shewanella (Gu *et al.*, 2024; Luo *et al.*, 2016). The simultaneous improvement in metabolic kinetics and interfacial charge transfer creates a steady operating condition for continuous power production. The interplay of these two elements creates an ideal bioelectrochemical environment for the sustained operation of MS-MFCs, as shown in Figure 6.

3.5. Implications for Marine Sediment MFC Design and Deployment

Analysis of electron transfer kinetics revealed that the incorporation of HC, especially at concentrations of 10–15%, elevated the electron transfer rate constant to over 3.0 s^{-1} on Day 30, markedly exceeding the rate of the unmodified system (1.77 s^{-1}). A raised k_s signifies less interfacial kinetic resistance in the bioelectrochemical system. This suggests that porous conductive materials may diminish kinetic resistance, enhance electrode-biofilm integration, and sustain prolonged power generation (Leng *et al.*, 2021). In field applications, MS-MFCs must use composite electrodes or sediment modifications that improve conductivity, surface area, and biocompatibility, allowing them to endure environmental fluctuations and substrate availability (Ojha *et al.*, 2025).

From an ecological perspective, MS-MFCs provide environmental benefits by using a natural microbial consortia and endogenous organic matter as energy sources, hence obviating the need for external chemical additions. The use of in situ substrates facilitates steady-state functioning with minimum external bulk and energy input. This device adheres to sustainable engineering principles and utilizes natural redox gradients in sediments to produce power with minimum effect. Its scalability facilitates implementation as modules implanted in rivers, wetlands, or marine sediments to produce energy in situ, hence facilitating decentralized and cost-effective energy systems (Walter *et al.*, 2020).

In contrast to alternative benthic energy harvesting technologies like lithium, piezoelectric, or thermoelectric batteries, MS-MFCs provide the distinct benefit of uninterrupted operation without requiring component replacement, avoiding contamination risks, and lacking reliance

on unstable thermal gradients in natural settings (Melchor-Martínez *et al*., 2021; Tian *et al*., 2024). This operating simplicity lowers long-term system resistance and maintenance requirements. Despite having a lower power density than commercial batteries, MS-MFCs are adequate for powering low-energy sensors, wireless data loggers, and autonomous monitoring systems in wetland and coastal environments (Rahimnejad, 2023). Consequently, MS-MFCs are more suitably regarded as maintenance-free energy sources for prolonged monitoring systems instead of as substitutes for high-capacity energy storage (Algar *et al*., 2020).

4. Conclusion

The present study shows that the co-modification of MS-MFCs with hydrochar and acetate synergistically enhances electron transfer kinetics and charge storage capacitance via a combination of physicochemical processes and microbiological responses. The combined effects directly illustrate the interaction between interfacial reaction kinetics and transport processes that dictate energy conversion efficiency in heterogeneous electrochemical systems. The incorporation of HC elevates sediment conductivity and diminishes ohmic losses, while simultaneously providing redox-active groups, mainly quinones and phenolics, that expedite faradic charge transfer and augment pseudocapacitive contributions to the electrodes. Acetate serves as an easily available substrate, promoting the metabolism of electroactive bacteria and maintaining local redox conditions, therefore expediting EET. The integration of these two processes elevates the electron transfer rate constant from 1.77 to over 3.0 s^{-1} and enhances the maximum power to over 23 mW m^{-2}, representing a gain of three orders of magnitude compared to the unmodified system. The findings validate that the establishment of a conductive percolation network, redox mediation via surface groups, and increased microbial activity are essential factors in improving the efficacy of natural sediment-based MS-MFCs. These results provide a molecular framework for comprehending how HC operates as both a dual conductivity enhancer and a nutrient adsorbent, hence affecting biofilms and redox microhabitats in the long run. Future efforts must incorporate the analysis of microbial community dynamics, in situ characterization of ion/electron transport, and long-term field testing to enhance the utilization of HC as a sustainable material in benthic bioenergy systems and to augment its reliability in marine and estuarine environments.

Acknowledgments

The authors gratefully acknowledge the support provided by the Department of Chemistry and the Master of Energy Program, Universitas Diponegoro. Their academic facilities, technical assistance, and research environment were essential for the successful completion of this study.

Supplementary data

The supplementary information of this article can be accessed in https://ijred.cbiore.id/index.php/ijred/article/downloadSuppFile/62325/16143

Author Contributions: Marcelinus Christwardana: Funding Acquisition, Conceptualization, Methodology, Writing- Original draft preparation, Writing- Reviewing and Editing. Dilla Dayanti: Investigation, Software, Writing- Original draft preparation. Yayuk Astuti: Visualization, Data curation, Writing- Reviewing and Editing. H. Hadiyanto: Data curation, Supervision, Writing- Reviewing and Editing. K. Khoirunnisa: Data curation, Validation. Achmad Yanuar Maulana: Investigation, Data curation, Writing- Original draft preparation, Writing- Reviewing and Editing. Keisya Natania Nur A'intan: Data curation, Investigation.

Funding: This study was fully funded by Universitas Diponegoro through DIPA (Selain APBN) 2025 under the Riset Publikasi Internasional Bereputasi Tinggi (RPIBT) scheme (Contract No. 222-683/UN7.D2/PP/IV/2025)

Conflicts of Interest: The authors declare no conflict of interest.

References

Abazarian, E., Gheshlaghi, R., & Mahdavi, M. A. (2023). Interactions between sediment microbial fuel cells and voltage loss in series connection in open channels. *Fuel,* 332. https://doi.org/10.1016/j.fuel.2022.126028

Algar, C. K., Howard, A., Ward, C., & Wanger, G. (2020). Sediment microbial fuel cells as a barrier to sulfide accumulation and their potential for sediment remediation beneath aquaculture pens. *Scientific Reports*, 10(1). https://doi.org/10.1038/s41598-020-70002-4

Babauta, J., Renslow, R., Lewandowski, Z., & Beyenal, H. (2012). Electrochemically active biofilms: facts and fiction. A review. *Biofouling,* 28(8), 789-812. https://doi.org/10.1080/08927014.2012.710324

Caizán-Juanarena, L., Borsje, C., Sleutels, T., Yntema, D., Santoro, C., Ieropoulos, I., Soavi, F., & ter Heijne, A. (2020). Combination of bioelectrochemical systems and electrochemical capacitors: Principles, analysis and opportunities. *Biotechnology Advances*, 39. https://doi.org/10.1016/j.biotechadv.2019.107456

Chen, S., He, Y., Li, Q., Deng, X., Kang, B., He, Y., Lu, Y., Chen, J., & Su, C. (2025). Enhancing microbial fuel cell-expanded granular sludge bed for treating sulfate-containing wastewater by adding biochar and hydrochar: Performance and potential mechanisms. *Bioresource Technology*, 437. https://doi.org/10.1016/j.biortech.2025.133064

Christwardana, M., Fauziah, Z., & Sarjono, P. R. (2024). Investigating the influence of Saccharomyces cerevisiae on microbial fuel cell performance through bioelectrochemical and biochemical approaches under varied operating conditions. *Biomass Conversion and Biorefinery*. 15, 8189–8202; https://doi.org/10.1007/s13399-024-05734-8

Christwardana, M., Suedy, S. W. A., Harmoko, U., Malika, A., & Dayanti, D. (2025). Carbonization and aromaticity-driven electron transfer in hydrochars from tropical woods as electrochemical cell electrode for energy conversion and storage. *Bioresource Technology Report*s, 30. https://doi.org/10.1016/j.biteb.2025.102107

Dang, C. H., Cappai, G., Chung, J. W., Jeong, C., Kulli, B., Marchelli, F., Ro, K. S., & Román, S. (2024). Research Needs and Pathways to Advance Hydrothermal Carbonization Technology. *Agronomy*,14(2). https://doi.org/10.3390/agronomy14020247

De Schamphelaire, L., Rabaey, K., Boeckx, P., Boon, N., & Verstraete, W. (2008). Outlook for benefits of sediment microbial fuel cells with two bio-electrodes. *Microbial Biotechnology*, 1(6),. 446–462). https://doi.org/10.1111/j.1751-7915.2008.00042.x

Delgado, Y., Tapia, N., Muñoz-Morales, M., Ramirez, Á., Llanos, J., Vargas, I., & Fernández-Morales, F. J. (2024). Effect of hydrochar-doping on the performance of carbon felt as anodic electrode in microbial fuel cells. *Environmental Science and Pollution Research,* 32(49), 28253-28265. https://doi.org/10.1007/s11356-024-33338-2

Eckermann, A. L., Feld, D. J., Shaw, J. A., & Meade, T. J. (2010). Electrochemistry of redox-active self-assembled monolayers. *Coordination chemistry reviews*, 254(15-16), 1769-1802. https://doi.org/10.1016/j.ccr.2009.12.023

Elgrishi, N., Rountree, K. J., McCarthy, B. D., Rountree, E. S., Eisenhart, T. T., & Dempsey, J. L. (2018). A practical beginner's guide to cyclic voltammetry. *Journal of chemical education*, 95(2), 197-206. http://dx.doi.org/10.1021/acs.jchemed.7b00361

Fan, X., Zhou, Y., Jin, X., Song, R. B., Li, Z., & Zhang, Q. (2021). Carbon material-based anodes in the microbial fuel cells. *Carbon Energy,* 3(3), 449-472. https://doi.org/10.1002/cey2.113

Feng, Y., Du, H., Wulandari, T., Poinern, G. E. J., Jiang, Z. T., Fawcett, D., Hassan, N., Xue, L., & Yang, L. (2022). Hydrochar amendments stimulate soil nitrous oxide emission by increasing production of hydroxyl radicals and shifting nitrogen functional genes in the short term: A culture experiment. *Chemosphere*, 302. https://doi.org/10.1016/j.chemosphere.2022.134771

Gong, G., Wu, B., Liu, L., Li, J., Zhu, Q., He, M., & Hu, G. (2022). Metabolic engineering using acetate as a promising building block for the production of bio-based chemicals. *Engineering Microbiology,* 2(4). https://doi.org/10.1016/j.engmic.2022.100036

Gu, P., Li, F., Huang, Z., & Gao, J. (2024). Application of Acetate as a Substrate for the Production of Value-Added Chemicals in Escherichia coli. *Microorganisms*, 12(2). https://doi.org/10.3390/microorganisms12020309

Gupta, D., Mahajani, S. M., & Garg, A. (2021). Hydrothermal carbonization of household wet waste – characterization of hydrochar and process wastewater stream. *Bioresource Technology*, 342. https://doi.org/10.1016/j.biortech.2021.125972

Han, Y., Luo, Y., Zhang, L., Lu, X., Luo, X., Wu, X., & Zan, F. (2025). Deciphering the mechanistic insight into modified biochar for distinct anaerobic digestion processes: Surface functional groups and electron-transmitting capabilities. *Journal of Environmental Chemical Engineering,* 13(2). https://doi.org/10.1016/j.jece.2025.115581

Harnisch, F., & Freguia, S. (2012). A basic tutorial on cyclic voltammetry for the investigation of electroactive microbial biofilms. *Chemistry–An Asian Journal,* 7(3), 466-475. https://doi.org/10.1002/asia.201100740

Heenen, H. H., Shin, H., Kastlunger, G., Overa, S., Gauthier, J. A., Jiao, F., & Chan, K. (2022). The mechanism for acetate formation in electrochemical CO(2) reduction on Cu: selectivity with potential, pH, and nanostructuring. *Energy and Environmental Science*, 15(9), 3978–3990. https://doi.org/10.1039/d2ee01485h

Helder, M., Strik, D. P. B. T. B., Hamelers, H. V. M., Kuijken, R. C. P., & Buisman, C. J. N. (2012). New plant-growth medium for increased power output of the Plant-Microbial Fuel Cell. *Bioresource Technology,* 104, 417–423. https://doi.org/10.1016/j.biortech.2011.11.005

Hou, B., Hu, Y.-Y., Sun, J., & Cao, Y.-Q. (2010). Effect of anodic biofilm growth on the performance of the microbial fuel cell (MFC). 4th *International Conference on Bioinformatics and Biomedical Engineering*, 1–4.

Huang, Q., Liu, Y., & Dhar, B. R. (2024). Deciphering the microbial interactions and metabolic shifts at different COD/sulfate ratios in electro-assisted anaerobic digestion. *Journal of Hazardous Materials*, 480. https://doi.org/10.1016/j.jhazmat.2024.135801

Hubenova, Y., Bardarov, I., Hubenova, E., & Slavcheva, E. (2024). Sediment microbial fuel cells capable of powering outdoor environmental monitoring sensors. *Sensing and Bio-Sensing Research,* 46. https://doi.org/10.1016/j.sbsr.2024.100695

Ji, L., Yu, Z., Cao, Q., Gui, X., Fan, X., Wei, C., Jiang, F., Wang, J., Meng, F., Li, F., & Wang, J. (2024). Effect of hydrothermal temperature on the optical properties of hydrochar-derived dissolved organic matter and their interactions with copper (II). *Biochar*, 6(1). https://doi.org/10.1007/s42773-024-00353-y

Laviron, E. J. J. (1979). General expression of the linear potential sweep voltammogram in the case of diffusionless electrochemical systems. *Journal of Electroanalytical Chemistry and Interfacial Electrochemistry*, 101(1), 19-28. https://doi.org/10.1016/S0022-0728(79)80075-3

Lee, Y. S., An, J., Kim, B., Park, H. J., Kim, J., & Chang, I. S. (2015). Increased power in sediment microbial fuel cell: Facilitated mass transfer via a water-layer anode embedded in sediment. *PLoS ONE*, 10(12). https://doi.org/10.1371/journal.pone.0145430

Leng, L., Xiong, Q., Yang, L., Li, H., Zhou, Y., Zhang, W., Jiang, S., Li, H., & Huang, H. (2021). An overview on engineering the surface area and porosity of biochar. *Science of the Total Environment,* 763.. https://doi.org/10.1016/j.scitotenv.2020.144204

Liu, H., & Logan, B. E. (2004). Electricity generation using an air-cathode single chamber microbial fuel cell in the presence and absence of a proton exchange membrane. *Environmental Science and Technology,* 38(14), 4040–4046. https://doi.org/10.1021/es0499344

Luo, H., Yu, S., Liu, G., Zhang, R., & Teng, W. (2016). Effect of in-situ immobilized anode on performance of the microbial fuel cell with high concentration of sodium acetate. *Fuel,* 182, 732–739. https://doi.org/10.1016/j.fuel.2016.06.032

Marsili, E., Rollefson, J. B., Baron, D. B., Hozalski, R. M., & Bond, D. R. (2008). Microbial biofilm voltammetry: direct electrochemical characterization of catalytic electrode-attached biofilms. *Applied and environmental microbiology,* 74(23), 7329-7337. https://doi.org/10.1128/AEM.00177-08

Marzban, N., Libra, J. A., Ro, K. S., Moloeznik Paniagua, D., Rotter, V. S., Sturm, B., & Filonenko, S. (2024). Hydrochar stability: understanding the role of moisture, time and temperature in its physiochemical changes. *Biochar,* 6(1). https://doi.org/10.1007/s42773-024-00329-y

Mathis, T. S., Kurra, N., Wang, X., Pinto, D., Simon, P., & Gogotsi, Y. (2019). Energy storage data reporting in perspective—guidelines for interpreting the performance of electrochemical energy storage systems. *Advanced Energy Materials*, 9(39), 1902007. https://doi.org/10.1002/aenm.201902007

Matsuzaki, C., Takagi, H., Saiga, S., Kinoshita, Y., Yamaguchi, M., Higashimura, Y., & Yamamoto, K. (2024). Prebiotic effect of galacto-N-biose on the intestinal lactic acid bacteria as enhancer of acetate production and hypothetical colonization. *Applied and Environmental Microbiology,* 90(3). https://doi.org/10.1128/aem.01445-23

Melchor-Martínez, E. M., Macias-Garbett, R., Malacara-Becerra, A., Iqbal, H. M. N., Sosa-Hernández, J. E., & Parra-Saldívar, R. (2021). Environmental impact of emerging contaminants from battery waste: A mini review. *Case Studies in Chemical and Environmental Engineering*, 3. https://doi.org/10.1016/j.cscee.2021.100104

Mitov, M., Bardarov, I., Mandjukov, P., & Hubenova, Y. (2015). Chemometrical assessment of the electrical parameters obtained by long-term operating freshwater sediment microbial fuel cells. *Bioelectrochemistry,* 106, 105–114. https://doi.org/10.1016/j.bioelechem.2015.05.017

Mosali, V. S. S., Soucie, H., Peng, X., Faegh, E., Elam, M., Street, I., & Mustain, W. E. (2025). Mechanistic insights into the electrochemical oxidation of acetate at noble metals. *Chem Catalysis*, 5(2), 101190. https://doi.org/10.1016/j.checat.2024.101190

Mutyala, S., & Kim, J. R. (2022). Recent advances and challenges in the bioconversion of acetate to value-added chemicals. *Bioresource Technology,* 364. https://doi.org/10.1016/j.biortech.2022.128064

Nagarajan, T., Veilumuthu, P., Srinithan, T., & Christopher, J. G. (2025). An Introduction to Mangrove Ecosystem and Their Associated Microorganisms. In S. Muthusamy, R. Manikkam, & G. Venugopal (Eds.), Mangrove Microbiome: Diversity and Bioprospecting (pp. 3–18). Springer Nature Singapore. https://doi.org/10.1007/978-981-96-2602-1_1

Nourbakhsh, F., Pazouki, M., & Mohsennia, M. (2020). Simultaneous investigation of three effective parameters of substrate, microorganism type and reactor design on power generation in a dual-chamber microbial fuel cells. *Iranian Journal of Biotechnology,* 18(2), 1–29. https://doi.org/10.30498/ijb.2020.132869.2292

Ojha, R., Dash, J., Satpathy, S. S., Ojha, P. C., & Pradhan, D. (2025). A brief review on factors affecting the performance of microbial fuel cell and integration of artificial intelligence. *Discover Sustainability,* 6(1). https://doi.org/10.1007/s43621-025-01619-6

Padhye, L. P., Bandala, E. R., Wijesiri, B., Goonetilleke, A., & Bolan, N. (2022). Hydrochar: A Promising Step Towards Achieving a Circular Economy and Sustainable Development Goals. *Frontiers in Chemical Engineering,* 4. https://doi.org/10.3389/fceng.2022.867228

Pilz, F. H., & Kielb, P. (2023). Cyclic voltammetry, square wave voltammetry or electrochemical impedance spectroscopy? Interrogating electrochemical approaches for the determination of electron transfer rates of immobilized redox proteins. *BBA advances,* 4, 100095. https://doi.org/10.1016/j.bbadva.2023.100095

Puig, S., Serra, M., Coma, M., Cabré, M., Balaguer, M. D., & Colprim, J. (2010). Effect of pH on nutrient dynamics and electricity production using microbial fuel cells. *Bioresource Technology*, 101(24), 9594–9599. https://doi.org/10.1016/j.biortech.2010.07.082

Quintana-Najera, J., Blacker, A. J., Fletcher, L. A., & Ross, A. B. (2021). The effect of augmentation of biochar and hydrochar in anaerobic digestion of a model substrate. *Bioresource Technology*, 321. https://doi.org/10.1016/j.biortech.2020.124494

Rafiee, M., Abrams, D. J., Cardinale, L., Goss, Z., Romero-Arenas, A., & Stahl, S. S. (2024). Cyclic voltammetry and chronoamperometry: mechanistic tools for organic electrosynthesis. Chemical Society Reviews, 53(2), 566–585). https://doi.org/10.1039/d2cs00706a

Rahimnejad, M. (2023). Chapter 9 - MFCs' challenges and their potential solutions. In M. Rahimnejad (Ed.), Biological Fuel Cells (pp. 225–248). Elsevier. https://doi.org/10.1016/B978-0-323-85711-6.00007-2

Sharma, S., & Chand, P. (2023). Supercapacitor and electrochemical techniques: A brief review. *Results in Chemistry*, 5. https://doi.org/10.1016/j.rechem.2023.100885

Suliborska, K., Baranowska, M., Bartoszek, A., Chrzanowski, W., & Namieśnik, J. (2019). Determination of Antioxidant Activity of Vitamin C by Voltammetric Methods. *Proceedings* , *11*(1), 23. https://doi.org/10.3390/proceedings2019011023

Sun, J., Zhang, S., & Luo, G. (2023). The Role of Hydrochar in Promoting Methane Production from Anaerobic Digestion with Different Inocula. *Fermentation,* 9(5). https://doi.org/10.3390/fermentation9050433

Sun, T., Levin, B. D. A., Guzman, J. J. L., Enders, A., Muller, D. A., Angenent, L. T., & Lehmann, J. (2017). Rapid electron transfer by the carbon matrix in natural pyrogenic carbon. *Nature Communications*, 8. https://doi.org/10.1038/ncomms14873

Taherzadeh, D., Picioreanu, C., & Horn, H. (2012). Mass transfer enhancement in moving biofilm structures. *Biophysical Journal*, 102(7), 1483–1492. https://doi.org/10.1016/j.bpj.2012.02.033

Tang, K., Li, S., Luo, Y., Feng, W., Zhang, Z., Wang, L., Zhao, H., Chen, X., Li, X., & Wu, Z. (2025). Integrating metagenomics and untargeted metabolomics to analyze the relationship between microbial dynamics and non-volatile metabolomic profiles in plant-derived microbial fuel cells (MFCs). *RSC Advances*, 15(25), 19582–19597. https://doi.org/10.1039/d5ra01080b

Teng, S.-X., Tong, Z.-H., Li, W.-W., Wang, S.-G., Sheng, G.-P., Shi, X.-Y., Liu, X.-W., & Yu, H.-Q. (2010). Electricity generation from mixed volatile fatty acids using microbial fuel cells. *Applied Microbiology and Biotechnology*, 87(6), 2365–2372. https://doi.org/10.1007/s00253-010-2746-5

Thunshirn, P., Wenzel, W. W., & Pfeifer, C. (2022). Pore characteristics of hydrochars and their role as a vector for soil bacteria: A critical review of engineering options. *Critical Reviews in Environmental Science and Technology*, 52(23), 4147–4171).. https://doi.org/10.1080/10643389.2021.1974256

Tian, Y., Ren, G. K., Wei, Z., Zheng, Z., Deng, S., Ma, L., Li, Y., Zhou, Z., Chen, X., Shi, Y., & Lin, Y. H. (2024). Advances of thermoelectric power generation for room temperature: Applications, devices, materials and beyond. *Renewable Energy,* 226. https://doi.org/10.1016/j.renene.2024.120443

Walter, X. A., Santoro, C., Greenman, J., & Ieropoulos, I. A. (2020). Scalability and stacking of self-stratifying microbial fuel cells treating urine. *Bioelectrochemistry,* 133. https://doi.org/10.1016/j.bioelechem.2020.107491

Wang, X., Wu, Y., Chen, N., Piao, H., Sun, D., Ratnaweera, H., Maletskyi, Z., & Bi, X. (2022). Characterization of Oxidation-Reduction Potential Variations in Biological Wastewater Treatment Processes: A Study from Mechanism to Application. *Processes,* 10(12). https://doi.org/10.3390/pr10122607

Wei, Y. M., Kumar, K. D., Zhang, L., & Li, J. F. (2025). Pseudocapacitive materials for energy storage: properties, mechanisms, and applications in supercapacitors and batteries. *Frontiers in Chemistry*, 13. https://doi.org/10.3389/fchem.2025.1636683

Xu, Q., Yang, G., Liu, X., Wong, J. W. C., & Zhao, J. (2023). Hydrochar mediated anaerobic digestion of bio-wastes: Advances, mechanisms and perspectives. *Science of the Total Environment,* 884. https://doi.org/10.1016/j.scitotenv.2023.163829

Xu, Y., Ou, Q., Zhou, X., He, Q., Wu, Z., Huang, R., Song, J., Ma, J., & Huangfu, X. (2020). Impacts of carrier properties, environmental conditions and extracellular polymeric substances on biofilm formation of sieved fine particles from activated sludge. *Science of the Total Environment,* 731. https://doi.org/10.1016/j.scitotenv.2020.139196

Yan, T., Zhang, Z., Zhang, Z., Wang, W., Li, D., Zhang, T., & Zhu, Z. (2024). Applying Hydrochar Affects Soil Carbon Dynamics by Altering the Characteristics of Soil Aggregates and Microbes. *Agronomy*, 14(5). https://doi.org/10.3390/agronomy14051015

Yang, X., & Chen, S. (2021). Microorganisms in sediment microbial fuel cells: Ecological niche, microbial response, and environmental function. *Science of The Total Environment*, 756, 144145. https://doi.org/10.1016/j.scitotenv.2020.144145

Yang, X., Ma, X., Wang, K., Wu, D., Lei, Z., & Feng, C. (2016). Eighteen-month assessment of 3D graphene oxide aerogel-modified 3D graphite fiber brush electrode as a high-performance microbial fuel cell anode. *Electrochimica Acta,* 210, 846–853. https://doi.org/10.1016/j.electacta.2016.05.215

Zhang, P., Zhang, J., Zhang, T., Chen, J., Yang, Q., He, Y., & Tong, Y. W. (2025). Unraveling the electron hopping mechanism in biochar-enhanced syntrophic acetate oxidation for methane production. *Waste Management,* 204. https://doi.org/10.1016/j.wasman.2025.114925

Zhou, C., Fu, Y., Zhang, H., Chen, W., Liu, Z., Liu, Z., Ying, M., & Zai, X. (2018). Structure design and performance comparison of large-scale marine sediment microbial fuel cells in lab and real sea as power source to drive monitoring instruments for long-term work. *Ionics,* 24(3), 797–805. https://doi.org/10.1007/s11581-017-2251-2

Zhu, K., Xu, Y., Yang, X., Fu, W., Dang, W., Yuan, J., & Wang, Z. (2022). Sludge derived carbon modified anode in microbial fuel cell for performance improvement and microbial community dynamics. *Membranes,* 12(2), 120. https://doi.org/10.3390/membranes12020120